processes

Supplementary Information

A Selection Flowchart for Micromodel Experiments based on Computational Fluid Dynamic Simulations of Surfactant Flooding in Enhanced Oil Recovery

Santiago Céspedes [1,2], Alejandro Molina [2], Betiana Lerner [3,4], Maximiliano S. Pérez [3,4], Camilo A. Franco [1] and Farid B. Cortés[1,*]

1 Grupo de Investigación en Fénomenos de Superficie-Michael Polanyi, Department of Processes and Energy, Faculty of Mines, National University of Colombia, Medellín 050034, Colombia; sacespedeszu@unal.edu.co (S.C.); caafrancoar@unal.edu.co (C.A.F.); fbcortes@unal.edu.co (F.B.C.)
2 Grupo de Investigación Bioprocesos y Flujos Reactivos, Department of Processes and Energy, Faculty of Mines, National University of Colombia, Medellín 050034, Colombia; amolinao@unal.edu.co (A. M.).
3 Universidad Tecnológica Nacional (UTN), Facultad Regional Haedo, Haedo, Buenos Aires E 1706, Argentina; betianalerner@gmail.com (B.L.); max@fullgen.com.ar (M.S.P.)
4 Department of Electrical and Computer Engineering, Florida International University, Miami, Florida 33174, USA; betianalerner@gmail.com (B.L.); max@fullgen.com.ar (M.S.P.)

* Correspondence: e-mail@e-mail.com; Tel.: (optional; include country code; if there are multiple corresponding authors, add author initials)

Citation: Céspedes, S.; Molina, A.; Lerner, B.; Pérez, M.S.; Franco, C.A. A Selection Flowchart for Micromodel Experiments based on Computational Fluid Dynamic Simulations of Surfactant Flooding in Enhanced Oil Recovery. *Processes* **2021**, *9*, 1887. https://doi.org/10.3390/pr9111887

Academic Editor: Alfredo Iranzo

Received: 21 September 2021
Accepted: 8 October 2021
Published: 22 October 2021

S1. Meshing of the geometries

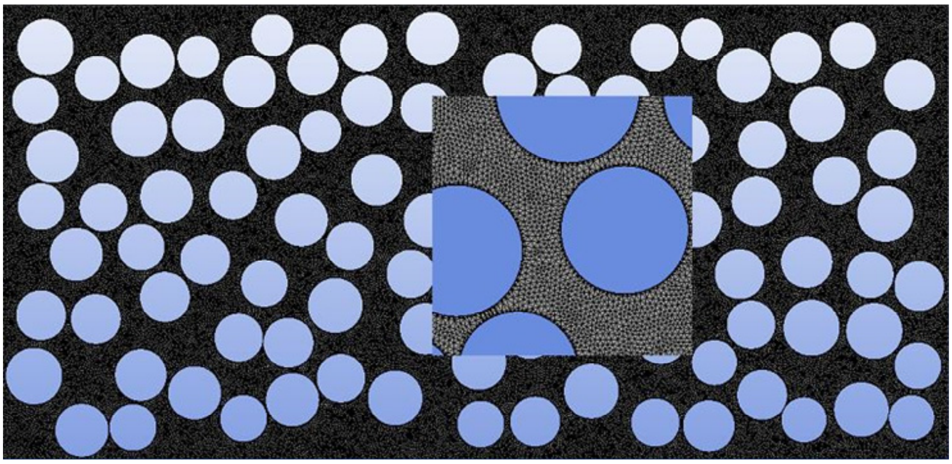

Figure S1. Detail of the mesh for micromodel (a)

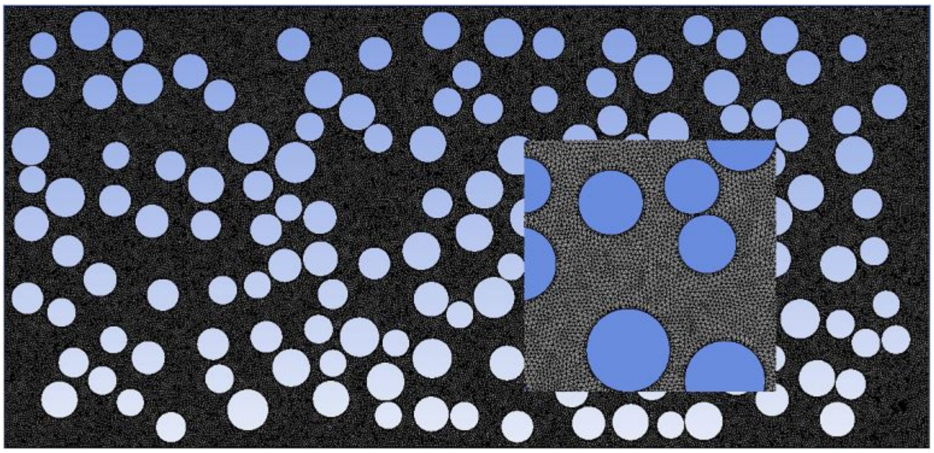

Figure S2. Detail of the mesh for micromodel (b).

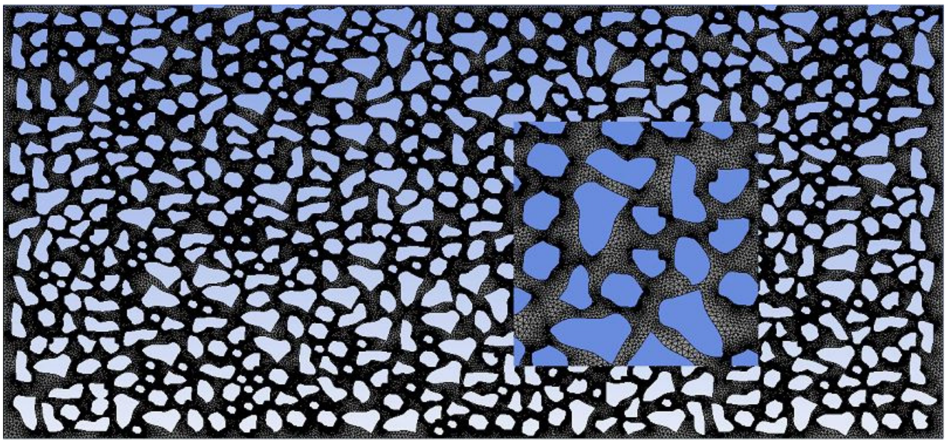

Figure S3. Detail of the mesh for micromodel (c)

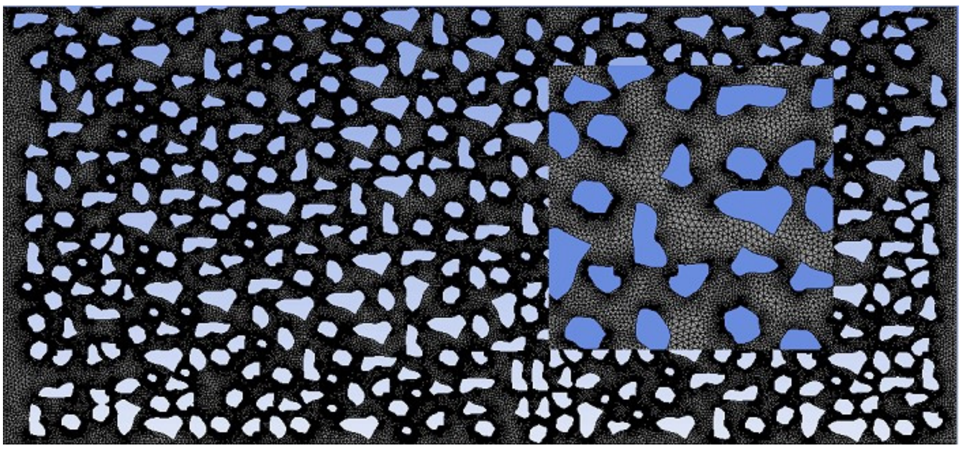

Figure S4. Detail of the mesh for micromodel (d)

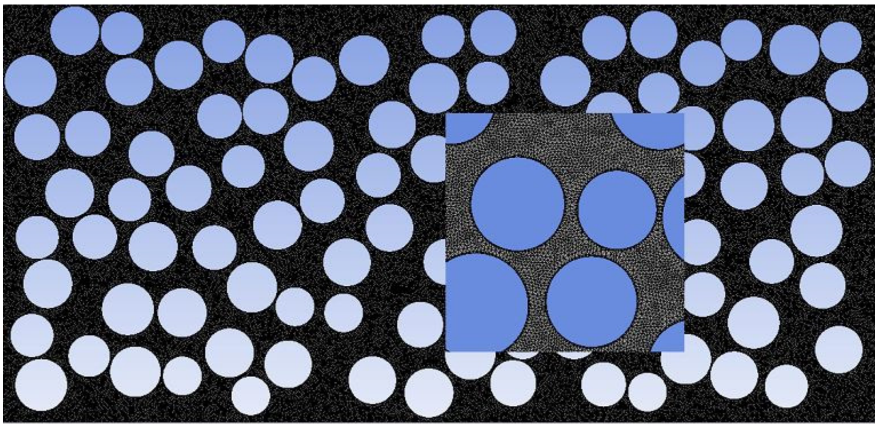

Figure S5. Detail of the mesh for micromodel (e)

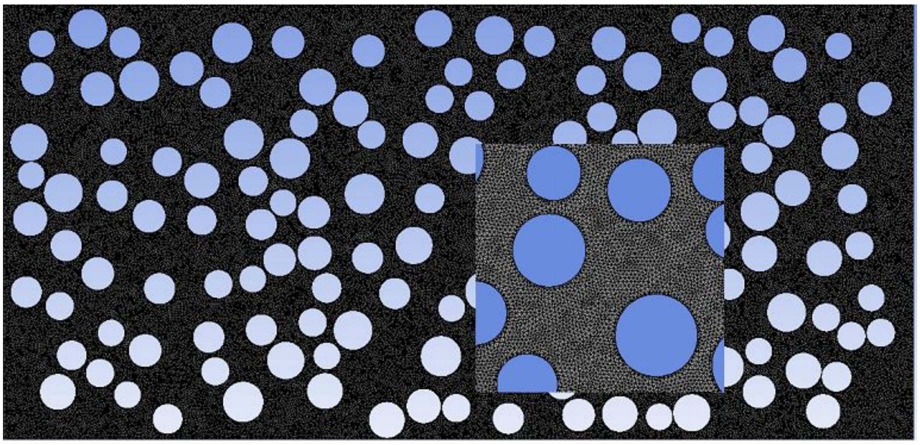

Figure S6. Detail of the mesh for micromodel (f)

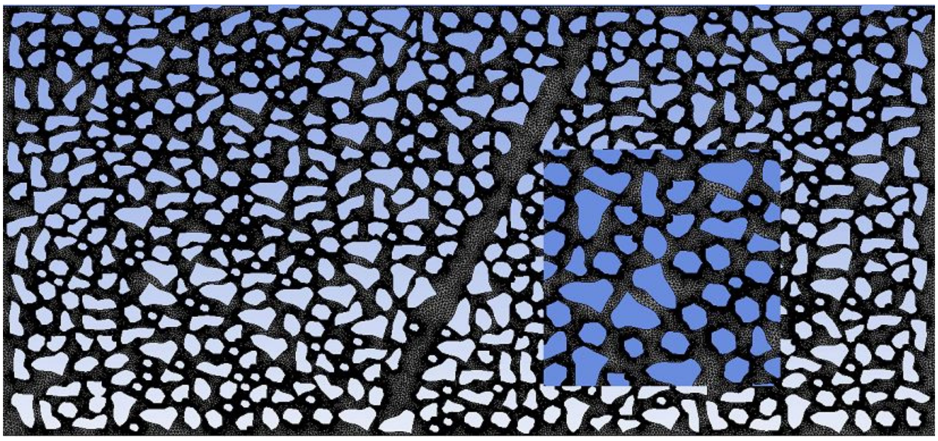

Figure S7. Detail of the mesh for micromodel (g)

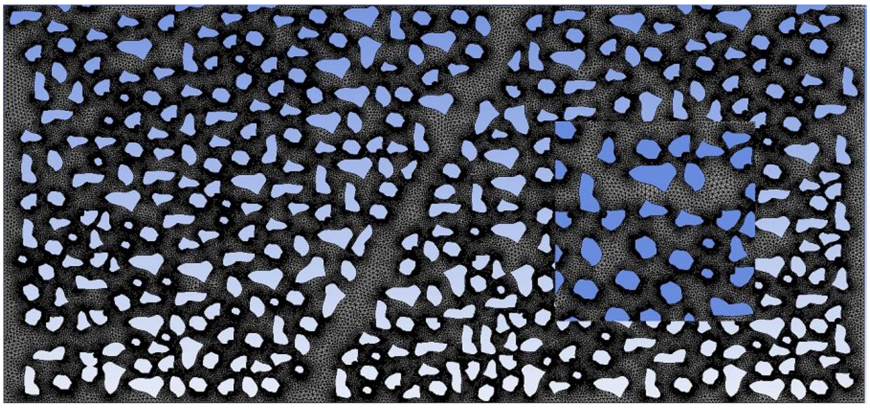

Figure S8. Detail of the mesh for micromodel (h)

S2. Parameters of the variable time step algorithm

A variable-time-step algorithm was used in all simulations with a global Courant number of 2. Table s.1 presents the parameters used for the variable-time-step algorithm.

Table S1. Parameters for the variable time-step algorithm used in the simulations.

Parameter	Value
Minimum Time Step Size (s)	0.0001
Maximum Time Step Size (s)	10
Minimum Step change factor	0.8
Maximum Step change factor	1.2
Initial Time Step size (s)	0.1

S3. Fractal dimension of the flow pattern

The fractal dimension of the flow pattern at the breakthrough time was computed based on image analysis and the fractal box-counting method [1], where a series of boxes of decreasing size are systematically laid over the flow pattern, and the number of these elements (*N*) in each sequence is determined. The fractal dimension is obtained from the slope of the line of the plot of the logarithm of *N* and the logarithm of the inverse of the box size (*r*) as described by Equation S1.

$$D = \frac{log(N)}{\log(r)} \quad \text{(S1)}$$

where *D* is the fractal dimension of the analyzed pattern.

S4. Phase behavior

Phase behavior and its modeling are also considered in this research. Figure s.9 represents the phase behavior between crude oil and surfactant solution.

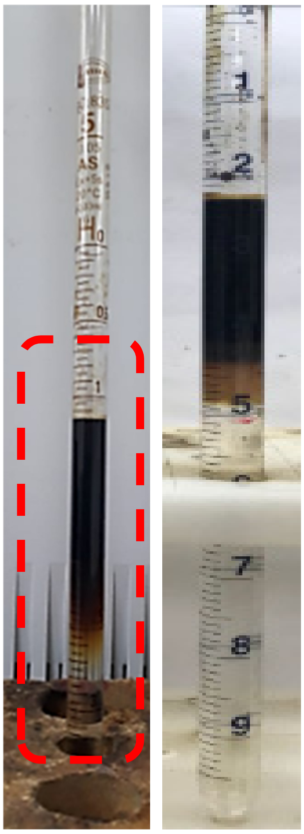

Figure S9. Phase behavior between crude oil and surfactant solution.

As can be seen in Figure s.9, there is a type III Winsor behavior between the phases, where a petroleum microemulsion is formed in a separate phase between the petroleum and water phases. In this case, the system comprises a surfactant solution displacing microemulsion, which displaces oil [2,3]. Despite the knowledge of the behavior of phases, in the modeling, the implication of considering two phases mobilizing through the micromodel is carried out, this is done in order to simplify the mathematical model, where the basis of additional research carried out with similar phenomenology was taken [4-7].

S4. Extensive Selection Flowchart

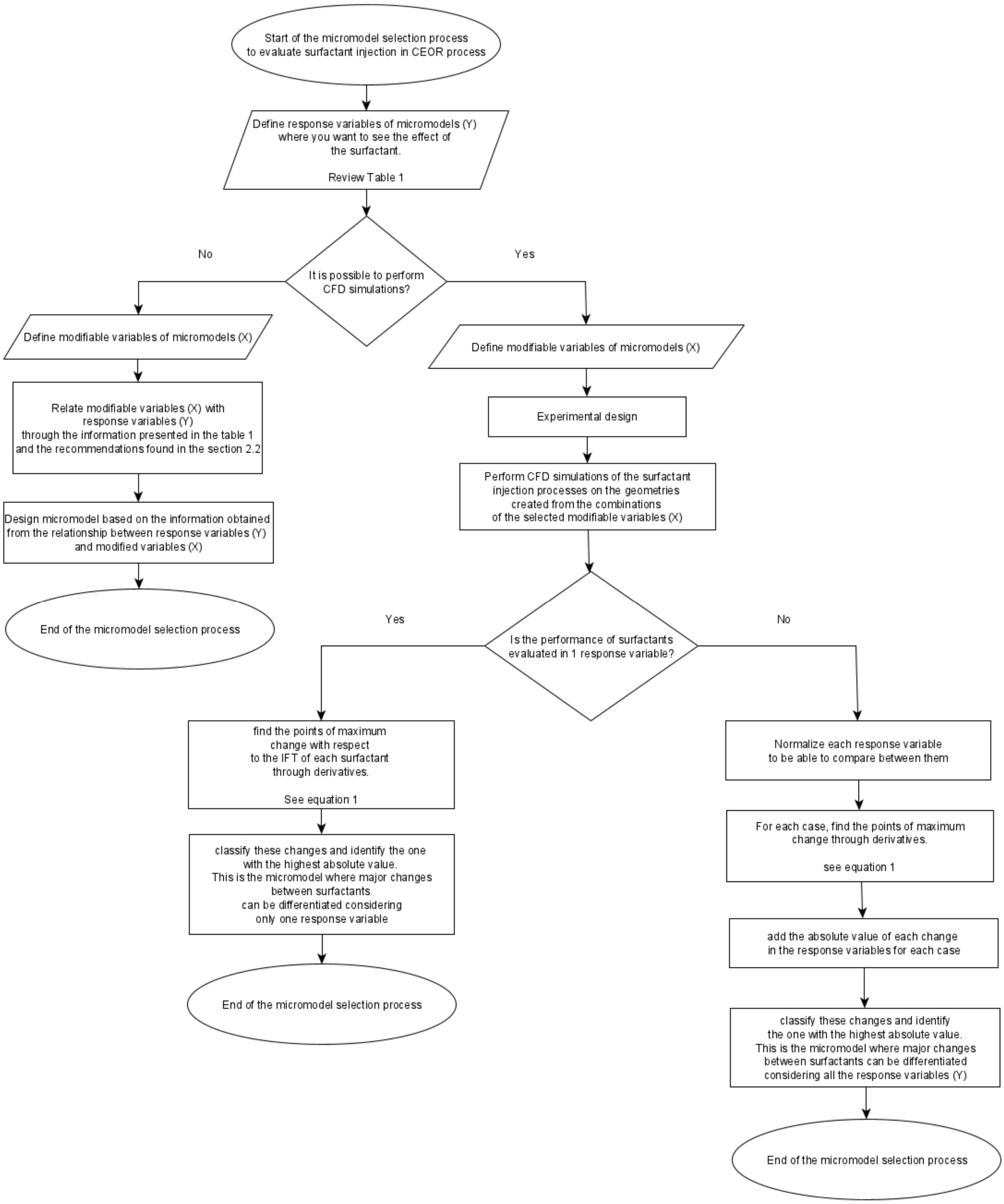

Figure S10. Extensive Selection Flowchart for micromodel experiments.

References

1. Falconer, K. *Fractal geometry: mathematical foundations and applications*; John Wiley & Sons: 2004.
2. Alzahid, Y.A.; Mostaghimi, P.; Walsh, S.D.; Armstrong, R.T. Flow regimes during surfactant flooding: The influence of phase behaviour. *Fuel* **2019**, *236*, 851-860.
3. Kegel, W.; Lekkerkerker, H. Phase behaviour of an ionic microemulsion system as a function of the cosurfactant chain length. *Colloids and Surfaces A: Physicochemical and Engineering Aspects* **1993**, *76*, 241-248.
4. Rostami, P.; Sharifi, M.; Aminshahidy, B.; Fahimpour, J. The effect of nanoparticles on wettability alteration for enhanced oil recovery: micromodel experimental studies and CFD simulation. *Petroleum Science* **2019**, *16*, 859–873.
5. Gharibshahi, R.; Jafari, A.; Ahmadi, H. CFD investigation of enhanced extra-heavy oil recovery using metallic nanoparticles/steam injection in a micromodel with random pore distribution. *Journal of Petroleum Science and Engineering* **2019**, *174*, 374-383, doi:doi.org/10.1016/j.petrol.2018.10.051.
6. Ghanad Dezfully, M.; Jafari, A.; Gharibshahi, R. CFD simulation of enhanced oil recovery using nanosilica/supercritical CO2. *Advanced Materials Research* **2015**, *1104*, 81-86, doi:doi.org/10.4028/www.scientific.net/AMR.1104.81.
7. Gharibshahi, R.; Jafari, A.; Haghtalab, A.; Karambeigi, M.S. Application of CFD to evaluate the pore morphology effect on nanofluid flooding for enhanced oil recovery. *RSC Advances* **2015**, *5*, 28938-28949.